Spin-dipole mode in a trapped Fermi gas near unitarity

Hiroyuki Tajima,[1] Alessio Recati,[2,3] and Yoji Ohashi[4]
[1]*Quantum Hadron Physics Laboratory, RIKEN Nishina Center (RNC), Wako, Saitama 351-0198, Japan*
[2]*INO-CNR BEC Center and Dipartimento di Fisica, Università di Trento, 38123 Povo, Italy*
[3]*Trento Institute for Fundamental Physics and Applications, INFN, 38123 Trento, Italy*
[4]*Department of Physics, Keio University, Hiyoshi, Kohoku-ku, Yokohama 223-8522, Japan*

(Received 25 September 2019; published 13 January 2020)

We theoretically investigate the spin-dipole oscillation of a strongly interacting Fermi gas confined by a harmonic trapping potential. By using a diagrammatic strong-coupling theory combined with a local density approximation and a sum rule approach, we study the temperature dependence of the spin-dipole frequency near unitarity. The connection of the spin-dipole frequency with the spin susceptibility and the pairing correlations is exploited. While the spin-dipole frequency exactly coincides with the trap frequency in a noninteracting Fermi gas, it is shown to be strongly enhanced in the superfluid state, because of the suppression of the spin degree of freedom due to the spin-singlet Cooper-pair formation. In strongly interacting Fermi gases, such enhancement occurs even above the superfluid phase transition temperature, due to the strong pairing correlations.

DOI: 10.1103/PhysRevA.101.013610

I. INTRODUCTION

Ultracold atomic gases have emerged as an ideal testing ground for the study of strongly correlated systems [1–4]. The most remarkable feature of this system is the possibility of modifying the interatomic interaction using Feshbach resonances [5], that has allowed one to examine various strong-coupling phenomena in Fermi gases.

In particular, unitary Fermi gases, where the scattering length a_s is adjusted to be divergent ($a_s = \pm\infty$) [6–9], have attracted much attention because of its universal property. Whereas the unitary Fermi gas does not depend on any scales associated with the interaction, the presence of strong pairing fluctuations is anticipated. Indeed, the photoemission spectrum measurements near the superfluid critical temperature T_c indicate the existence of the pseudogap in single-particle excitations [10–13], originating from strong pairing fluctuations in the Bardeen-Cooper-Schrieffer (BCS) -Bose-Einstein condensation (BEC) crossover regime (for a review, see Refs. [14,15]). On the other hand, it has also been shown that the observed equation of state in a unitary Fermi gas can be well reproduced by the Fermi liquid theory, without including strong pairing fluctuations [16]. Therefore it is desirable to consider other quantities that are sensitive to pairing fluctuations in order to understand the strongly interacting regime.

Since the formation of singlet pairs suppresses the spin degrees of freedom, the spin susceptibility is a promising candidate for this purpose, and, e.g., the so-called spin-gap phenomenon, where the spin susceptibility is suppressed in the pseudogap regime, has been predicted [17–21]. While the spin susceptibility has been recently experimentally accessed in cold Fermi gas physics [22,23], this many-body phenomenon has not been observed yet. Furthermore, the spin-dipole frequency [24,25], which is also deeply related to the inverse of the spin susceptibility, has been experimentally observed and been successfully employed to observe the ferromagnetic behavior in the upper energy branch of a repulsive Fermi gas [26]. In Ref. [26] the measurement of the spin-dipole frequency in the (attractive) lower energy branch is also reported. While the spin-dipole frequency in a noninteracting Fermi gas is equal to the trap frequency due to Kohn's theorem with respect to the dipole mode even at finite temperatures [27,28], a large enhancement of this frequency has been observed in the unitary regime due to the reduction of spin susceptibility.

Another interesting aspect of the spin-dipole mode is its analogy with the giant dipole resonance (GDR) in nuclei [29]. In such nuclear systems, the strong neutron-proton interaction plays an important role. The excitation-energy dependence of GDR has been investigated to see the effects of collective motions, as well as thermodynamic properties of excited nuclei [30].

In this work, we discuss the spin-dipole frequency in an attractively interacting Fermi gas in a harmonic trap, by using a combined extended T-matrix approximation (ETMA) [31] with a local density approximation (LDA) and a sum-rule approach. Such a diagrammatic approach can not only reproduce the observed spin susceptibility, but also connect the spin susceptibility with pairing-fluctuation corrections in a homogeneous two-component Fermi gas [20,21]. In particular, the single-particle density of states obtained from ETMA exhibits the pseudogap phenomenon near T_c, where the spin susceptibility is suppressed due to the formation of spin-singlet preformed Cooper pairs. We also note that ETMA can successfully describe the recently observed ground-state thermodynamic quantities [32–34], as well as the spin polarization [35], in the unitary regime. The ETMA gives the Bertsch parameter $\xi = 0.38$, superfluid gap $\Delta = 0.44\varepsilon_F$, and Tan's contact $C = 0.098k_F^4$ in a unitary Fermi gas at $T = 0$ [32] (where ε_F and k_F are the Fermi energy and momenta, respectively). It also gives the superfluid critical temperature $T_c = 0.20T_F$ (where T_F is the Fermi temperature). These ETMA

results agree with the recent experiments [9,13,36–38], as well as quantum Monte Carlo simulations [19,39–42]. Using this strong-coupling theory, we clarify the effects of strong pairing interactions on the spin-dipole frequency in a strongly interacting trapped Fermi gas. We also compare our numerical results with the recent experiment done near the unitarity limit.

This paper is organized as follows. In Sec. II, we explain our theoretical framework for the spin-dipole mode in a trapped Fermi gas. In Sec. III, we discuss strong-coupling corrections on the spin-dipole frequency. In what follows, we take $\hbar = k_{\rm B} = 1$.

II. FORMALISM

We start by considering a homogeneous three-dimensional two-component Fermi gas with a contact-type interaction. The Hamiltonian is given by

$$H = \sum_{\sigma=\uparrow,\downarrow}\sum_{\boldsymbol{p}}(\xi_{\boldsymbol{p}} - \sigma h)c^{\dagger}_{\boldsymbol{p},\sigma}c_{\boldsymbol{p},\sigma} - U\sum_{\boldsymbol{p},\boldsymbol{k},\boldsymbol{q}} c^{\dagger}_{\boldsymbol{p}+\boldsymbol{q}/2,\uparrow}c^{\dagger}_{-\boldsymbol{p}+\boldsymbol{q}/2,\downarrow}c_{-\boldsymbol{k}+\boldsymbol{q}/2,\downarrow}c_{\boldsymbol{k}+\boldsymbol{q}/2,\uparrow}, \quad (1)$$

where $c_{\boldsymbol{p},\sigma}$ ($c^{\dagger}_{\boldsymbol{p},\sigma}$) is the annihilation (creation) operator of a Fermi atom with momentum $\boldsymbol{p}$ and pseudospin σ, $\xi_{\boldsymbol{p}} = p^2/(2m) - \mu$ the kinetic energy (m being the atomic mass) measured from the chemical potential μ, and h an effective magnetic field, i.e., (twice) the difference of the chemical potentials between the $\sigma = \uparrow$ and $\downarrow$ components. The interaction strength $-U$ is related to the s-wave scattering length a_s as

$$U = \left[\sum_{\boldsymbol{p}}^{|\boldsymbol{p}|\leqslant p_{\rm c}} \frac{m}{p^2} - \frac{m}{4\pi a_s}\right]^{-1}, \quad (2)$$

where $p_{\rm c}$ is the cut-off momentum. In order to study the superfluid phase we introduce the superfluid order parameter Δ, to rewrite the model Hamiltonian in Eq. (1) as [43]

$$H = \sum_{\boldsymbol{p}} \psi^{\dagger}_{\boldsymbol{p}}[\xi_{\boldsymbol{p}}\tau_3 - h - \Delta\tau_1]\psi_{\boldsymbol{p}} - U\sum_{\boldsymbol{q}}\rho_{\boldsymbol{q},+}\rho_{\boldsymbol{q},-}, \quad (3)$$

where $\psi_{\boldsymbol{p}} = (c_{\boldsymbol{p},\uparrow}, c^{\dagger}_{-\boldsymbol{p},\downarrow})^{\rm t}$ is the two-component Nambu field [43], $\tau_{i=0,1,2,3}$ the Pauli matrice,s and $\rho_{\boldsymbol{q},\pm} = \sum_{\boldsymbol{p}}\psi^{\dagger}_{\boldsymbol{p}+\boldsymbol{q}/2}\tau_{\pm}\psi_{-\boldsymbol{p}+\boldsymbol{q}/2}$ are the generalized density operators with $\tau_{\pm} = (\tau_1 \pm i\tau_2)/2$.

As mentioned in the Introduction, we include the effects of a harmonic trap within LDA. In the present case of spin-independent trap potential $V(r) = \frac{1}{2}m\omega_{\rm tr}^2 r^2$, in LDA the chemical potential is simply given by [1]

$$\mu(r) = \mu - \tfrac{1}{2}m\omega_{\rm tr}^2 r^2, \quad (4)$$

where $\omega_{\rm tr}$ is the trap frequency. Note that h is position independent in this case. All the other quantities acquire spatial dependence via local solutions using Eq. (3). Introducing $\xi_{\boldsymbol{p}}(r) = \xi_{\boldsymbol{p}} + m\omega_{\rm tr}^2 r^2/2$, as well as the spatial-dependent order parameter, $\Delta \to \Delta(r)$, we define the 2×2 matrix LDA Green's function in the Nambu space as

$$\hat{G}_{\boldsymbol{p}}(i\omega_n, r)^{-1} = i\omega_n - \xi_{\boldsymbol{p}}(r)\tau_3 + h + \Delta(r)\tau_1 - \hat{\Sigma}_{\boldsymbol{p}}(i\omega_n, r), \quad (5)$$

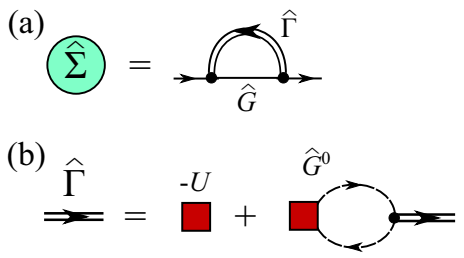

FIG. 1. Feynman diagram for the self-energy $\hat{\Sigma}$, as well as the many-body T matrix $\hat{\Gamma}$ (double solid lines). The box represents a contact-type attractive interaction $-U$. The solid and dashed lines show the dressed and bare Green's functions $\hat{G}$ and $\hat{G}^0$, respectively.

where $\omega_n = (2n+1)\pi T$ ($n \in \mathbb{Z}$) is the fermion Matsubara frequency. In ETMA, the LDA self-energy $\hat{\Sigma}_{\boldsymbol{p}}(i\omega_n, r)$ is diagrammatically described as Fig. 1(a), which gives

$$\hat{\Sigma}_{\boldsymbol{p}}(i\omega_n, r) = -T\sum_{\boldsymbol{q},i\zeta_{n'}}\sum_{j,j'=\pm}\Gamma^{j,j'}_{\boldsymbol{q}}(i\zeta_{n'}, r) \times \tau_j\hat{G}_{\boldsymbol{p}+\boldsymbol{q}}(i\omega_n + i\zeta_{n'}, r)\tau_{j'} \quad (6)$$

where $\zeta_{n'} = 2n'\pi T$ ($n' \in \mathbb{Z}$) is the boson Matsubara frequency. The LDA many-body T matrix $\hat{\Gamma}_{\boldsymbol{q}}(i\zeta_{n'}, r)$, diagrammatically shown in Fig. 1(b), has the form

$$\hat{\Gamma}_{\boldsymbol{q}}(i\zeta_{n'}, r) = -[1 + U\hat{\Pi}_{\boldsymbol{q}}(i\zeta_{n'}, r)]^{-1}U. \quad (7)$$

Here,

$$[\hat{\Pi}_{\boldsymbol{q}}(i\zeta_{n'}, r)]_{j,j'} = T\sum_{\boldsymbol{p},i\omega_n}{\rm tr}\big[\hat{G}^0_{\boldsymbol{p}+\boldsymbol{q}}(i\omega_n + i\zeta_{n'}, r) \times \tau_{j'}\hat{G}^0_{\boldsymbol{p}}(i\omega_n, r)\tau_j\big] \quad (8)$$

is the LDA pair-correlation matrix, where $\hat{G}^0_{\boldsymbol{p}}(i\omega_n, r) = [i\omega_n - \xi_{\boldsymbol{p}}(r)\tau_3 + \Delta(r)\tau_1]^{-1}$ is the bare BCS Green's function [3].

The local density $n_\sigma(r, T)$ is obtained from $\hat{G}_{\boldsymbol{p}}(i\omega_n)$ as

$$n_\uparrow(r, T) = T\sum_{\boldsymbol{p},i\omega_n}[\hat{G}_{\boldsymbol{p}}(i\omega_n, r)]_{11}e^{i\omega_n\delta}, \quad (9)$$

$$n_\downarrow(r, T) = T\sum_{\boldsymbol{p},i\omega_n}[\hat{G}_{\boldsymbol{p}}(i\omega_n, r)]_{22}e^{-i\omega_n\delta},$$

where δ is an infinitesimally small positive number. The Fermi chemical potential μ is determined by solving numerically the particle-number equation $N = N_\uparrow + N_\downarrow$ where

$$N_\sigma = \int d^3\boldsymbol{r}\, n_\sigma(r, T). \quad (10)$$

In the superfluid phase, we also determine the LDA superfluid order parameter $\Delta(r)$ from the gapless condition of the Nambu-Goldstone mode [44],

$$\det[1 + U\hat{\Pi}_{\boldsymbol{q}=0}(i\zeta_{n'} = 0, r)] = 0. \quad (11)$$

We define the LDA superfluid critical temperature $T_{\rm c}$ as the temperature below which $\Delta(r=0)$ becomes nonzero.

In the present work, we use the ETMA + LDA to estimate the spin-dipole mode frequency, i.e., the frequency of the out-of-phase in-trap dipole motion of the two spin components.

A rigorous upper bound [25] is given by the ratio between the energy weighted m_1 and the inverse energy weighted m_{-1} sum rules for the spin-dipole operator $\sum_i z_{i,\uparrow} - \sum_i z_{i,\downarrow}$, where the sums run over all the $\uparrow$ and $\downarrow$ atoms, respectively.

While $m_1 \propto N/m$, the sum rule m_{-1} directly depends on the magnetic susceptibility of the gas $\chi(r, T)$, which can be calculated as, in LDA,

$$\chi(r, T) = \lim_{h\to 0} \frac{n_\uparrow(r, T) - n_\downarrow(r, T)}{h}. \tag{12}$$

Eventually, the spin-dipole frequency $\omega_{\rm SD}$ is evaluated as [25]

$$\omega_{\rm SD}^2 \leqslant \frac{m_1}{m_{-1}} = \frac{N}{m \int d^3\boldsymbol{r}\, z^2 \chi(r, T)}. \tag{13}$$

In this work, we numerically evaluate Eq. (12) with a small magnetic field $h = 10^{-2}\varepsilon_{\rm F}$. As mentioned previously, h is actually not a real magnetic field, but the chemical potential difference between two components. While Eq. (13) generally represents an upper bound, it is expected to give a very accurate estimation for the spin-dipole frequency, since the spin-dipole operator excites mainly a single mode. We briefly note that, at low frequency, a better estimation can be obtained by including the mass normalization [25] in the f-sum rule as $m_1 \propto N/m^*$, which is, however, outside the scope of the present work, and which is a higher-order effect on the spin susceptibility along the temperature evolution. In the absence of interaction effects, since each spin component exhibits a dipole oscillation independently, the spin-dipole frequency coincides with the dipole frequency, i.e., due to Kohn's theorem [27,28], to the trap frequency. As we will also show in the following, the latter result is recovered in the presence of interaction at high enough temperature to make spin correlation negligible.

III. RESULTS

Figure 2 shows the temperature dependence of the spin-dipole frequency $\omega_{\rm SD}$ for a unitary Fermi gas in a harmonic trap. The solid and short-dashed lines represent the results of ETMA and the BCS mean-field approximation (hereinafter, referred to as BCS), respectively. The BCS result is obtained by solving Eq. (10) without the self-energy correction, namely, $\hat{\Sigma}_{\boldsymbol{p}}(i\omega_n, r) = 0$. Our result shows excellent agreement with the recent experiment at $T = 0.151T_{\rm F}$ [26], with $T_{\rm F} = (3N)^{1/3}\omega_{\rm tr}$ being the Fermi temperature in an ideal two-component Fermi gas. Although the experimental result was obtained in the condition that the two gas clouds of up and down spins are initially not fully overlapping, ETMA can quantitatively explain the magnetic properties of a unitary Fermi gas. A similar agreement about the strong-coupling corrections to the spin susceptibility have also been pointed out in Refs. [20,21].

As shown in Eq. (13), $\omega_{\rm SD}^2$ is inversely proportional to the *second moment* of the local spin susceptibility $\chi(r, T)$. Thus, $\omega_{\rm SD}$ becomes larger, for smaller $\chi(r, T)$. We obtain better insight into the large enhancement of $\omega_{\rm SD}$, from the spatial and temperature dependence of the local spin susceptibility $\chi(r, T)$. Figure 3 shows $\chi(r, T)$ as a function of r for different temperatures. We introduce the ideal Thomas-Fermi radius $R_{\rm F} = \sqrt{2\varepsilon_{\rm F}/(m\omega_{\rm tr}^2)}$ with $\varepsilon_{\rm F}$ the Fermi energy

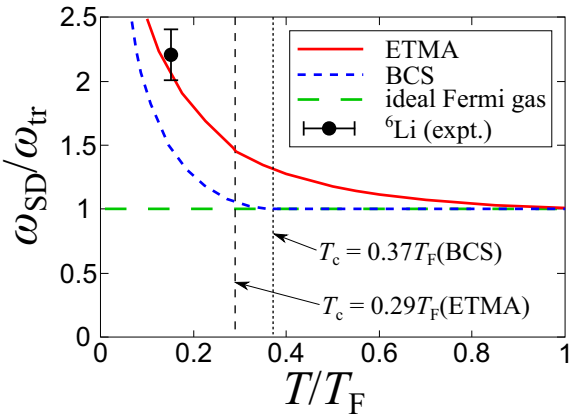

FIG. 2. Calculated spin-dipole frequency in a trapped unitary Fermi gas at finite temperature. The solid, dotted, and dashed lines represent the results of ETMA, BCS, and an ideal Fermi gas. The LDA critical temperatures of ETMA ($T_{\rm c} = 0.29T_{\rm F}$) and BCS ($T_{\rm c} = 0.37T_{\rm F}$) are shown, where $T_{\rm F} = (3N)^{1/3}\omega_{\rm tr}$ and $\omega_{\rm tr}$ are the Fermi temperature in a two-component ideal gas and the trap frequency, respectively. The black circle shows the recent experimental result on a ^{6}Li unitary Fermi gas [26].

of an ideal two-component Fermi gas at $T = 0$, as well as the local Pauli susceptibility, $\chi_0(r, T) = (3m/2)[n_\uparrow(r, T) + n_\downarrow(r, T)]^{1/3}/(3\pi^2)^{2/3}$ [46]. In the superfluid phase at $T = 0.1T_{\rm F}$ shown in Fig. 3(a1), both the ETMA and the BCS results exhibit peak structures. In our LDA formalism, the system forms a shell structure with a superfluid inner core [$\Delta(r) \neq 0$], surrounded by an outer normal region. The vertical dotted lines in Figs. 3(a1) and 3(a2) shows the boundary between the two phases.

In the superfluid region, the local spin susceptibility is largely suppressed due to the formation of singlet Cooper pairs, characterized by the LDA superfluid order parameter $\Delta(r)$ shown in the inset of Fig. 3(a2). While the ETMA result shows a larger $\chi(r, T)$ than that of BCS in the superfluid region, the opposite occurs in the normal region. This behavior reflects pairing fluctuations in each region. In particular, in the normal phase at $T = 0.4T_{\rm F}$ and $T = 0.8T_{\rm F}$ shown in Figs. 3(b1) and 3(c1), the ETMA result is always smaller than the BCS one. This difference originates from the formation of preformed Cooper pairs near $T_{\rm c}$ and the interaction effect becomes smaller at high temperature regime. For reference, we plot $n_\uparrow(r) + n_\downarrow(r)$ in Figs. 3(b2) and 3(c2) at each temperature in the normal phase.

We note that the calculation of BCS above $T_{\rm c}$ ($= 0.37T_{\rm F}$) is equivalent to the noninteracting case. Regarding this, $\omega_{\rm SD}$ is always equal to $\omega_{\rm tr}$ above $T_{\rm c}$ in the mean-field approximation. It is consistent with the Bogoliubov-de Gennes calculation with the random-phase approximation [45] which shows $\omega_{\rm SD} \simeq \omega_{\rm tr}$ in the normal phase. This fact supports the validity of LDA. However, as shown in Figs. 3(b1) and 3(c1), $\chi(r, T)$ in the normal phase clearly has a temperature dependence even in the mean-field calculation. Although the effects of pairing fluctuations on the trap-averaged spin susceptibility is unclear due to the fact that it involves not only pairing correlations, but also temperature-dependent density profile

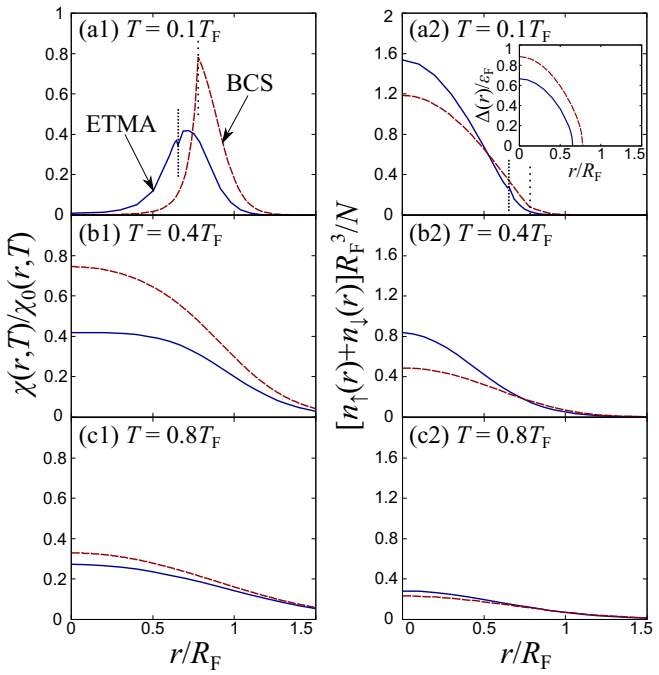

FIG. 3. Local spin susceptibility $\chi(r, T)$ at (a1) $T = 0.1T_F$ (superfluid phase), (b1) $T = 0.4T_F$, and (c1) $T = 0.8T_F$ in a trapped unitary Fermi gas. (a2), (b2), and (c2) show the corresponding local densities $n_\uparrow(r) + n_\downarrow(r)$. The inset in (a2) shows the LDA superfluid order parameter $\Delta(r)$. The solid and dashed lines represent the results of the ETMA and of the mean-field BCS theory, respectively. $\chi_0(r, T)$ is the Pauli susceptibility in a homogeneous gas with the number density $n_\sigma(r, T)$ (see text). The vertical dotted lines indicate the boundary between the normal state and the superfluid state in each calculation.

[46], the spin-dipole frequency is not affected by the latter effect.

In Fig. 4, we report the temperature dependence of the spin-dipole frequency away from unitarity. In the high-temperature limit, the expected result $\omega_{SD} = \omega_{tr}$ is recovered, irrespective of the interaction strength. On the other hand, ω_{SD} diverges in the low-temperature limit for nonzero pairing interaction, where the spin susceptibility vanishes because of the singlet Cooper pairing. Since the spin susceptibility decreases for a larger pairing interaction, ω_{SD} increases with increasing $(k_F a_s)^{-1}$. In particular, ω_{SD} becomes very large in the strong-coupling regime $[(k_F a_s)^{-1} \gtrsim 0.5]$ where atoms form tightly bound molecules. Again, even in such a regime, we obtain $\omega_{SD} = \omega_{tr}$ for $T \gg E_b$, with $E_b = 1/(ma_s^2)$ the two-body binding energy at $r = 0$.

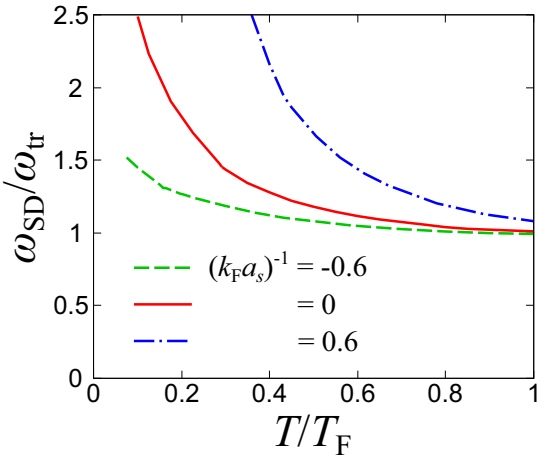

FIG. 4. Comparison of the spin-dipole frequencies at $(k_F a_s)^{-1} = -0.6$ (dashed line), 0 (solid line), and 0.6 (dot-dashed line). $k_F = \sqrt{2m\omega_{tr}(3N)^{1/3}}$ is the LDA Fermi momentum.

In this strong-coupling high-temperature regime, the system can simply be described by a classical atom-molecule mixture [46], so that the local spin susceptibility $\chi_{cl}(r, T)$ is analytically given by

$$\chi_{cl}(r, T) = \frac{2\lambda}{T}\left(\frac{mT}{2\pi}\right)^{3/2} \exp\left(-\frac{m\omega_{tr}^2 r^2}{2T}\right), \tag{14}$$

where $\lambda = e^{\mu/T}$ is the fugacity. Such a classical mixture model is equivalent to the so-called Saha-Langmuir equation [47,48]. Recently, the pair fraction predicted by the Saha-Langmuir equation shows good agreement with the cold-atom experiment in the BEC side [49]. Substituting Eq. (14) into Eq. (13), one obtains

$$\omega_{SD}^{cl} = \omega_{tr}\sqrt{\frac{1}{6\lambda}\left(\frac{T_F}{T}\right)^3}. \tag{15}$$

Since $\lambda = (T_F/T)^3/6$ in trapped ideal two-component gases, Eq. (15) is consistent with Kohn's theorem ($\omega_{SD}^{cl} = \omega_{tr}$). In the presence of the molecular bound state, λ is given by

$$\lambda = \frac{\sqrt{1 + \frac{2}{3}\left(\frac{T_F}{T}\right)^3 \exp(E_b/T)} - 1}{2\exp(E_b/T)}. \tag{16}$$

Using this, one can analytically obtain the spin-dipole frequency in the strong-coupling high-temperature limit,

$$\omega_{SD}^{cl} = \omega_{tr}\sqrt{\frac{\left(\frac{T_F}{T}\right)^3 \exp(E_b/T)}{3\sqrt{1 + \frac{2}{3}\left(\frac{T_F}{T}\right)^3 \exp(E_b/T)} - 3}}. \tag{17}$$

In this way, one can understand that the enhancement of ω_{SD} in the strong-coupling regime is due to the appearance of tightly bound molecules. Indeed, Eq. (17) coincides with Eq. (15) when $T \gg E_b$ because molecules are thermally dissociated. This result is in sharp contrast to the dipole mode which does not depend on the temperature and the interaction strength due to Kohn's theorem.

We summarize the phase diagram of an attractively interacting trapped Fermi gas from the viewpoint of the spin-dipole mode in Fig. 5. In this figure, we plot the temperatures where $\omega_{SD}/\omega_{tr} = 1.05$, 1.10, and 1.20. These three characteristic temperatures monotonically increase with increasing the pairing interaction strength. One can find the smooth crossover from the high-temperature region ("KM"), where the spin-dipole oscillation can be explained by the two independent Kohn (dipole) modes of the spin $\sigma = \uparrow$ and $\downarrow$ gas clouds, to the fast-oscillation region ("FO") where ω_{SD} largely deviates from ω_{tr} due to the strong attractive interaction. Although there is no clear phase boundary between KM and FO, this result indicates that ω_{SD} is sensitive to the pairing interaction, as well as resulting singlet-pair formations. For reference,

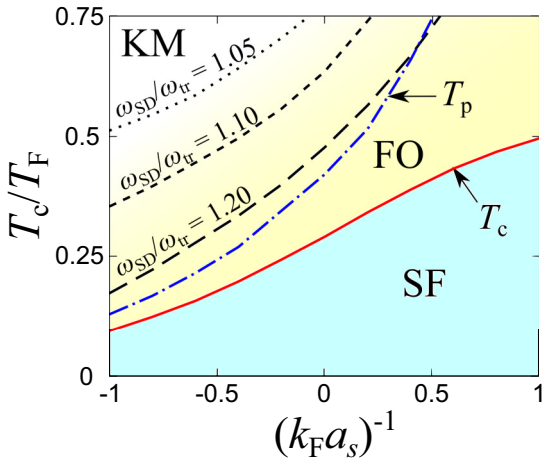

FIG. 5. Phase diagram of an attractively interacting trapped Fermi gas. The solid line shows the LDA superfluid critical temperature T_c, below which the system undergoes the superfluid phase ("SF"). While the spin-dipole frequency can be explained by the Kohn (dipole) mode in the high-temperature region ("KM"), it is strongly enhanced at low temperatures (fast oscillation region, "FO"). Although there are no clear boundaries between "KM" and "FO," the crossover between these two regimes can be characterized by the temperatures where $\omega_{SD}/\omega_{tr} = 1.05$ (dotted line), 1.10 (dashed line), and 1.20 (long-dashed line). For comparison, we also plot the peak temperature T_p of the trap-averaged spin susceptibility shown in [46].

we also show in Fig. 5 the peak temperature T_p of the trap-averaged spin susceptibility in an attractive Fermi gas in a harmonic trap [46]. T_p is close to the temperature where $\omega_{SD}/\omega_{tr} = 1.20$, in the entire crossover region.

Figure 6 shows ω_{SD}^{cl} at $T = T_p$ in the strong-coupling regime. T_p as a function of $(k_F a_s)^{-1}$ is also shown in the inset of Fig. 6. While T_p increases and ω_{SD}^{cl} at $T = T_p$ slightly decreases with increasing the binding energy, this indicates that the spin-dipole frequency starts to be enhanced when the

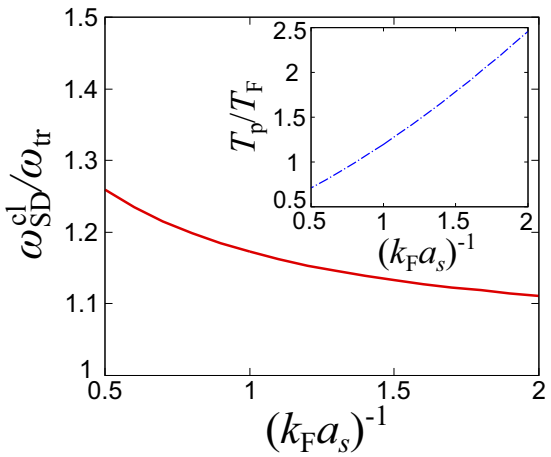

FIG. 6. Calculated spin-dipole frequency ω_{SD}^{cl} in the classical atom-molecule mixture at $T = T_p$. The inset shows the peak temperature T_p of the trap-averaged spin susceptibility [46], as a function of $(k_F a_s)^{-1}$, in the strong-coupling limit.

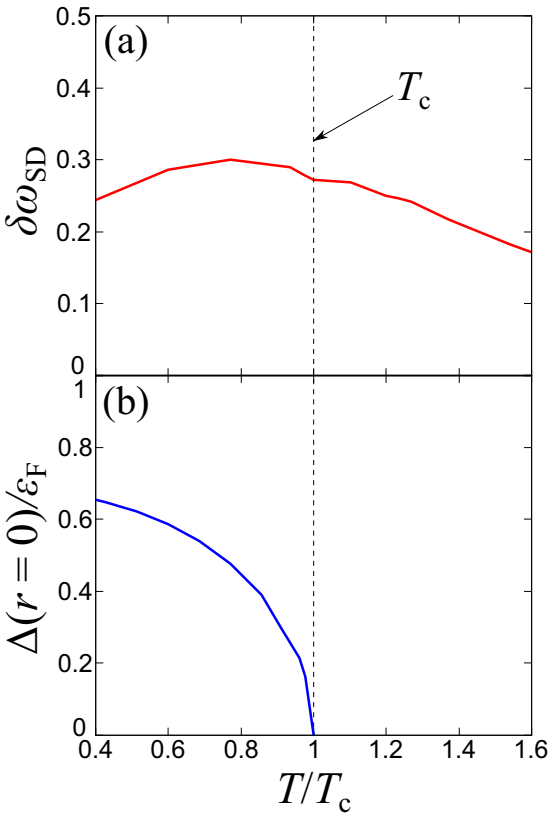

FIG. 7. (a) Calculated frequency shift $\delta\omega_{SD} = (\omega_{SD}^{ETMA} - \omega_{SD}^{BCS})/\omega_{SD}^{ETMA}$ due to the pairing correlations beyond the mean-field approximation near T_c. (b) LDA superfluid order parameter $\Delta(r = 0)$ in the trap center.

trap-averaged spin susceptibility is suppressed by the singlet-pair formation.

To see how the emergent superfluid order and pairing fluctuations affect the spin-dipole mode below T_c, we plot in Fig. 7(a) the frequency shift $\delta\omega_{SD} = (\omega_{SD}^{ETMA} - \omega_{SD}^{BCS})/\omega_{SD}^{ETMA}$ near T_c, where $\omega_{SD}^{ETMA(BCS)}$ is the spin-dipole frequency obtained by ETMA (BCS). For reference, we also plot the LDA superfluid order parameter $\Delta(r = 0)$ in the trap center in Fig. 7(b). By definition, this frequency shift $\delta\omega_{SD}$ purely originates from the pairing correlations beyond the mean-field level. $\delta\omega_{SD}$ gradually increases with decreasing temperature in the high-temperature region, and starts to decrease around $T = 0.77T_c = 0.23T_F$, where $\Delta(r = 0)$ largely evolves. The pairing effect on ω_{SD} is most visible near this temperature. Indeed, pairing fluctuations become strong near T_c in single-particle excitations [50–53]. Finally, in the low-temperature regime, $\delta\omega_{SD}$ becomes smaller, indicating that the spin-dipole oscillation can qualitatively be explained by the mean-field theory and pairing fluctuations are suppressed by the appearance of the superfluid order in this regime.

IV. SUMMARY

To summarize, we have studied the spin-dipole frequency in a trapped Fermi gas near the unitarity by using the extended T-matrix approximation combined with the local density

approximation and a sum-rule approach. We have shown that our numerical result is in excellent agreement with recent experimental results at unitarity. In the classical (high-temperature, strong-coupling) regime, the analytical expression for the spin-dipole frequency has been derived.

The spin-dipole frequency exhibits a large enhancement in the low-temperature regime, due to the formation of the spin-singlet pairs in the center of the trap, i.e., due to the formation of a sizable region of zero magnetic susceptibility. The spin-dipole frequency coincides with the trap frequency in the high-temperature regime, in agreement with Kohn's theorem. However, in the strong-coupling regime, where a molecular bound state is present, the spin-dipole frequency deviates from the trap frequency as long as $T \gtrsim E_{\rm b}$.

We have discussed the effect of strong pairing correlations on the spin-dipole mode and compare our ETMA + LDA results with the BCS + LDA calculation. As a future topic, it would be interesting to compare our results with a recent density functional theory within the asymmetric superfluid local density approximation [54,55], which reproduces ground-state properties of a unitary Fermi gas even in the presence of the population imbalance.

While this work focused on the mass-balanced case, our results could be generalized to mass-imbalanced systems. This is relevant for the new generation of Fermi-Fermi mixture experiment where the overlap of the two Fermi clouds can be large as in the case of disprosium-potassium mixtures [56,57]. Regarding this, we comment on the fact that the upper bound Eq. (13) could even be improved by considering that the low-energy quasiparticle excitations do not exhaust the f-sum rule m_1. While, for our equal mass case, the correction would be rather small, it could be an interesting future problem in mass-imbalanced mixtures.

ACKNOWLEDGMENTS

H.T. thanks K. Iida, F. Scazza, R. Hanai, M. Pini, and M. Ota for useful discussions. This work was supported by a Grant-in-Aid for JSPS fellows (Grant No. 17J03975). A.R. acknowledges support from the Provincia Autonoma di Trento and the FIS$\hbar$ project of the National Institute for Nuclear Physics. Y.O. was supported by a Grant-in-Aid for Scientific Research from MEXT and JSPS in Japan (Grants No. JP18K11345, No. JP18H05406, and No. JP19K03689).

[1] S. Giorgini, L. P. Pitaevskii, and S. Stringari, Rev. Mod. Phys. **80**, 1215 (2008).
[2] I. Bloch, J. Dalibard, and W. Zwerger, Rev. Mod. Phys. **80**, 885 (2008).
[3] G. C. Strinati, P. Pieri, G. Röpke, P. Schuck, and M. Urban, Phys. Rep. **738**, 1 (2018).
[4] Y. Ohashi, H. Tajima, and P. van Wyk, Prog. Part. Nucl. Phys., (2019) 103739.
[5] C. Chin, R. Grimm, P. Julienne, and E. Tiesinga, Rev. Mod. Phys. **82**, 1225 (2010).
[6] T.-L. Ho, Phys. Rev. Lett. **92**, 090402 (2004).
[7] S. Nascimbène, N. Navon, K. J. Jiang, F. Chevy, and C. Salomon, Nature (London) **463**, 1057 (2010).
[8] M. Horikoshi, S. Nakajima, M. Ueda, and T. Mukaiyama, Science **327**, 442 (2010).
[9] M. J. H. Ku, A. T. Sommer, L. W. Cheuk, and M. W. Zwierlein, Science **335**, 563 (2012).
[10] J. T. Stewart, J. P. Gaebler, and D. S. Jin, Nature (London) **454**, 744 (2008).
[11] J. P. Gaebler, J. T. Stewart, T. E. Drake, D. S. Jin, A. Perali, P. Pieri, and G. C. Strinati, Nat. Phys. **6**, 569 (2010).
[12] A. Perali, F. Palestini, P. Pieri, G. C. Strinati, J. T. Stewart, J. P. Gaebler, T. E. Drake, and D. S. Jin, Phys. Rev. Lett. **106**, 060402 (2011).
[13] Y. Sagi, T. E. Drake, R. Paudel, R. Chapurin, and D. S. Jin, Phys. Rev. Lett. **114**, 075301 (2015).
[14] E. Mueller, Rep. Prog. Phys. **80**, 104401 (2017).
[15] S. Jensen, C. N. Gilbreth, and Y. Alhassid, Eur. Phys. J.: Spec. Top. **227**, 2241 (2019).
[16] S. Nascimbène, N. Navon, S. Pilati, F. Chevy, S. Giorgini, A. Georges, and C. Salomon, Phys. Rev. Lett. **106**, 215303 (2011).
[17] T. Enss and R. Haussmann, Phys. Rev. Lett. **109**, 195303 (2012).
[18] F. Palestini, P. Pieri, and G. C. Strinati, Phys. Rev. Lett. **108**, 080401 (2012).
[19] G. Wlazłowski, P. Magierski, J. E. Drut, A. Bulgac, and K. J. Roche, Phys. Rev. Lett. **110**, 090401 (2013).
[20] H. Tajima, T. Kashimura, R. Hanai, R. Watanabe, and Y. Ohashi, Phys. Rev. A **89**, 033617 (2014).
[21] H. Tajima, R. Hanai, and Y. Ohashi, Phys. Rev. A **93**, 013610 (2016).
[22] C. Sanner, E. J. Su, A. Keshet, W. Huang, J. Gillen, R. Gommers, and W. Ketterle, Phys. Rev. Lett. **106**, 010402 (2011).
[23] A. Sommer, M. Ku, G. Roati, and M. W. Zwierlein, Nature (London) **472**, 201 (2011).
[24] L. Vichi and S. Stringari, Phys. Rev. A **60**, 4734 (1999).
[25] A. Recati and S. Stringari, Phys. Rev. Lett. **106**, 080402 (2011).
[26] G. Valtolina, F. Scazza, A. Amico, A. Burchianti, A. Recati, T. Enss, M. Inguscio, M. Zaccanti, and G. Roati, Nat. Phys. **13**, 704 (2017).
[27] W. Kohn, Phys. Rev. **123**, 1242 (1961).
[28] Y. Ohashi, Phys. Rev. A **70**, 063613 (2004).
[29] E. Lipparini and S. Stringari, Phys. Rep. **175**, 103 (1989).
[30] D. Santonocito, Y. Blumenfeld, C. Agodi, R. Alba, G. Bellia, R. Coniglione, F. Delaunay, A. Del Zoppo, P. Finocchiaro, N. Frascaria, F. Hongmei, V. Lima, C. Maiolino, E. Migneco, P. Piattelli, P. Sapienza, and J. A. Scarpaci, Nucl. Phys. A **788**, 215 (2007).
[31] T. Kashimura, R. Watanabe, and Y. Ohashi, Phys. Rev. A **86**, 043622 (2012).
[32] H. Tajima, P. van Wyk, R. Hanai, D. Kagamihara, D. Inotani, M. Horikoshi, and Y. Ohashi, Phys. Rev. A **95**, 043625 (2017).
[33] M. Horikoshi, M. Koashi, H. Tajima, Y. Ohashi, and M. Kuwata-Gonokami, Phys. Rev. X **7**, 041004 (2017).
[34] M. Horikoshi and M. Kuwata-Gonokami, Int. J. Mod. Phys. E **28**, 1930001 (2019).

[35] T. Kashimura, R. Watanabe, and Y. Ohashi, Phys. Rev. A **89**, 013618 (2014).
[36] A. Schirotzek, Y.-I. Shin, C. H. Schunck, and W. Ketterle, Phys. Rev. Lett. **101**, 140403 (2008).
[37] N. Navon, S. Nascimbène, F. Chevy, and C. Salomon, Science **328**, 729 (2010).
[38] S. Hoinka, P. Dyke, M. G. Lingham, J. J. Kinnunen, G. M. Bruun, and C. J. Vale, Nat. Phys. **13**, 943 (2017).
[39] A. Gezerlis and J. Carlson, Phys. Rev. C **77**, 032801(R) (2008).
[40] A. Bulgac, J. E. Drut, and P. Magierski, Phys. Rev. A **78**, 023625 (2008).
[41] S. Gandolfi, K. E. Schmidt, and J. Carlson, Phys. Rev. A **83**, 041601(R) (2011).
[42] Michael McNeil Forbes, S. Gandolfi, and A. Gezerlis, Phys. Rev. Lett. **106**, 235303 (2011).
[43] K. Y. M. Wong and S. Takada, Phys. Rev. B **37**, 5644 (1988).
[44] Y. Ohashi and A. Griffin, Phys. Rev. A **67**, 063612 (2003).
[45] G. M. Bruun and B. R. Mottelson, Phys. Rev. Lett. **87**, 270403 (2001).
[46] H. Tajima, R. Hanai, and Y. Ohashi, Phys. Rev. A **96**, 033614 (2017).
[47] M. N. Saha, Proc. R. Soc. A **99**, 135 (1921).
[48] K. H. Kingdon and I. Langmuir, Phys. Rev. **22**, 148 (1923).
[49] T. Paintner, D. K. Hoffmann, M. Jager, W. Limmer, W. Schoch, B. Deissler, M. Pini, P. Pieri, G. Calvanese Strinati, C. Chin, and J. Hecker Denschlag, Phys. Rev. A **99**, 053617 (2019).
[50] A. Perali, P. Pieri, G. C. Strinati, and C. Castellani, Phys. Rev. B **66**, 024510 (2002).
[51] S. Tsuchiya, R. Watanabe, and Y. Ohashi, Phys. Rev. A **80**, 033613 (2009).
[52] S. Tsuchiya, R. Watanabe, and Y. Ohashi, Phys. Rev. A **84**, 043647 (2011).
[53] M. Ota, H. Tajima, R. Hanai, D. Inotani, and Y. Ohashi, Phys. Rev. A **95**, 053623 (2017).
[54] A. Bulgac and Michael McNeil Forbes, Phys. Rev. Lett. **101**, 215301 (2008).
[55] *The BCS-BEC Crossover and the Unitary Fermi Gas*, Lecture Notes in Physics Vol. 836, edited by W. Zwerger (Springer-Verlag, Berlin/Heidelberg, 2012).
[56] C. Ravensbergen, V. Corre, E. Soave, M. Kreyer, E. Kirilov, and R. Grimm, Phys. Rev. A **98**, 063624 (2018).
[57] C. Ravensbergen, E. Soave, V. Corre, M. Kreyer, B. Huang, E. Kirilov, and R. Grimm, arXiv:1909.03424.